

Article

A Study on the Behavior Characteristics of Air Supply during Tunnel Fires under Natural Ventilation with Multiple Vertical Shafts

Lu He ^{1,*}, Yuyang Ming ¹, Ke Liao ¹, Haojun Zhang ¹, Chenhao Jia ¹, Guoqing Zhu ¹ and Haowen Tao ²

¹ School of Safety Engineering, China University of Mining and Technology, Xuzhou 221116, China; ts21120126p31@cumt.edu.cn (Y.M.); ts22120161p31@cumt.edu.cn (K.L.); ts22120103a31ld@cumt.edu.cn (H.Z.); ts22120149p31@cumt.edu.cn (C.J.)

² Department of fire protection, Southwest Jiaotong University, Chengdu 611756, China; haowen.tao@swjtu.edu.cn

* Correspondence: 6218@cumt.edu.cn

Abstract: This study investigates the behavior of air supply in tunnels with multiple vertical shafts during fire incidents, focusing on natural ventilation dynamics. Numerical simulation is utilized to analyze the effect of different variables on air supply within vertical shafts. The findings reveal that the position of the smoke front significantly influences the direction and flow rate of gases during fire development. The mass flow rate of air supply during the stable fire development stage is influenced by the geometric size and positioning of vertical shafts, with shafts closer to the fire source exhibiting higher air flow rates. To address this issue, this study introduces a predictive model for estimating air flow rates in vertical shafts. This model exhibits a high level of accuracy when compared to simulations, offering a reliable method for predicting air flow rates based on the geometric characteristics of vertical shafts. Overall, this research contributes to understanding the complexities of air supply in tunnels with multiple vertical shafts, aiding in the improvement of natural ventilation strategies during fire incidents.

Keywords: air supply; multiple vertical shafts; tunnel fire; smoke exhaust



Citation: He, L.; Ming, Y.; Liao, K.; Zhang, H.; Jia, C.; Zhu, G.; Tao, H. A Study on the Behavior Characteristics of Air Supply during Tunnel Fires under Natural Ventilation with Multiple Vertical Shafts. *Fire* **2023**, *6*, 393. <https://doi.org/10.3390/fire6100393>

Academic Editors: Fei Tang and Lizhong Yang

Received: 19 August 2023

Revised: 9 October 2023

Accepted: 10 October 2023

Published: 13 October 2023



Copyright: © 2023 by the authors. Licensee MDPI, Basel, Switzerland. This article is an open access article distributed under the terms and conditions of the Creative Commons Attribution (CC BY) license (<https://creativecommons.org/licenses/by/4.0/>).

1. Introduction

Tunnels are vital components of public transportation networks, but their potential to pose significant risks to human life and the economy during fire incidents cannot be overlooked [1–3]. The improvement of tunnel fire safety has become a matter of great academic and engineering concern as it directly impacts public safety and mitigates potential mass casualties and substantial financial losses.

Tunnel fires pose a very high threat to the safety of people and vehicles due to the small space, poor ventilation, and rapid fire spread in tunnels [4]. Various measures can be implemented to mitigate the risk of tunnel fires impacting individuals and vehicles, and among these measures is the utilization of natural ventilation. In tunnels, naturally ventilated shafts are becoming more popular as the primary method of transverse smoke exhaustion. Several studies have been undertaken to examine the behavior of air entrainment, smoke control, and tunnel fire ventilation performance, utilizing the geometries and configurations of multiple shafts.

Naturally ventilated shafts have gained increasing attention as the primary method for transverse smoke exhaustion in tunnels during fires. Several studies have explored different aspects of natural ventilation utilizing shafts. Ji et al. [5,6] investigated plug-holing and boundary-layer separation at various shaft heights, while Fan et al. [7] studied air entrainment and found that a significant portion of the exhausted rate was due to entrained air. The impact of vertical shaft positioning on the effectiveness of natural ventilation was

investigated by the researchers of [8]. Cong et al. [9] analyzed the flow mechanism within and around vertical shafts and developed a general formula to predict the dimensionless volume flow rates. The prediction equation for vertical shaft heat extract performance was established by He et al. [10], who introduced the Froude number as a representative parameter. Guo et al. [11,12] conducted tests on smoke spread in tunnels with large-sized shafts, and analyzed smoke movement, temperature distribution, and velocity of the smoke front. They also developed theoretical models for smoke mass flow rates [13]. Li et al. [14] developed updated temperature decay models for estimating smoke temperature decrease. Wang et al. [15] assessed the efficiency of natural multiple shafts for heat and smoke exhaust, emphasizing the importance of shaft aspect ratio and cross-sectional shape in achieving higher efficiency. Fan et al. [16] analyzed the fire suppression performance of a water mist system in railway fire scenarios and provided a significant reference for the design of water mist systems.

The investigations conducted by the above researchers have contributed to a better understanding of the behavior of natural ventilation performance, smoke control, and heat exhaust efficiency using naturally ventilated shafts in tunnels. Despite this, the majority of previous studies have focused on examining the temperature or smoke characteristics of certain shafts in tunnel fires, without accounting for the coupling impact of multiple shafts. Furthermore, the majority of previous studies have centered around the steady stage of tunnel fire, with inadequate emphasis on the laws governing smoke propagation during the fire development phase.

The natural smoke extraction process in tunnels with multiple vertical shafts aims to achieve effective smoke control by exhausting smoke outside the tunnels. Efficient removal of smoke is achieved by designing a natural ventilation system that takes into account the heat release rate (HRR) and strategically positioning vertical shafts near potential fire source. These vertical shafts have a fundamental role in smoke extraction, while the flow field within the tunnels adheres to the principle of mass conservation, thus ensuring efficient removal of smoke during the evacuation phase. Additionally, the portals at both ends of the tunnels and other vertical shafts that are not involved in smoke extraction act as air inlets during a fire incident. This configuration helps maintain the balance of airflow, thereby facilitating the removal of smoke from the tunnels. In some special scenarios, such as strong environmental winds outside the tunnels or rain, smoke may not be fully diluted after being discharged from vertical shafts and may remain at a low altitude. If the smoke plume spreads to the opening of a vertical shaft that is acting as an air supply, it can cause smoke to flow back.

During the fire development stage, when the smoke front extends toward the portals of a tunnel, the downward airflow originating from the vertical shafts intersects with the smoke ceiling jet at a perpendicular angle. The presence of this interaction disrupts smoke stratification and compromises the efficiency of smoke extraction through the vertical shafts. Consequently, the objective of this article is to examine the underlying mechanisms that govern the air supply behavior of vertical shafts in natural ventilation. Moreover, a predictive model for airflow at each tunnel opening is established. This article's findings and predictive model for air supply behavior in natural ventilation tunnels will support their design, thereby improving performance and safety during fire incidents.

2. Theoretical Analysis

This article investigates the distinct characteristics of smoke flow during various stages of tunnel fires, categorizing it into three stages. Using a horizontally oriented tunnel as an example, as shown in Figure 1, with a centrally located fire source, this study examines the smoke movement within symmetrically designed tunnels on either side of the fire source.

Stage 1: during the initial stage, smoke has not yet reached the first vertical shaft.

Stage 2: during the development stage, the smoke front progresses through multiple vertical shafts while continuing its forward spread.

Stage 3: during the stable stage, the smoke front remains stationary, and the vertical shafts engaged in smoke extraction maintain stability without any alterations to the mass flow rate.

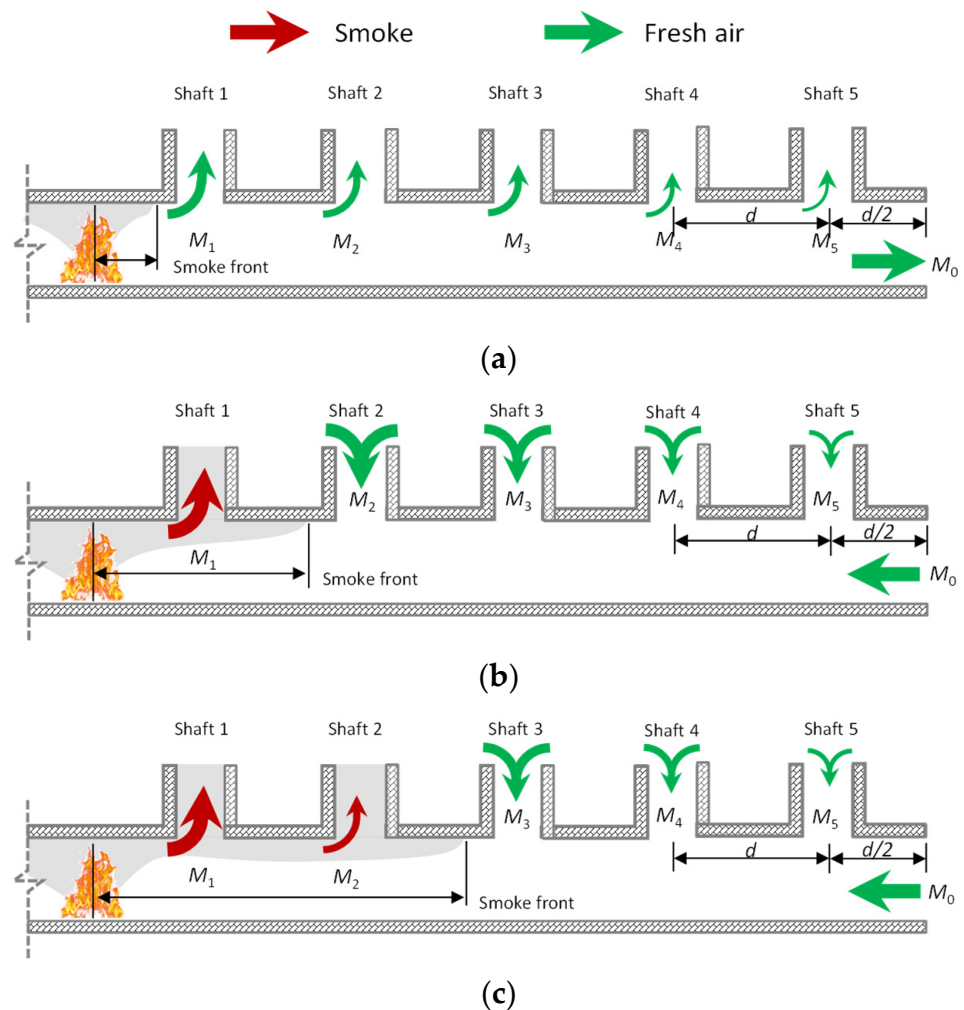


Figure 1. Variations in the tunnel flow field during different fire development stages: (a) stage 1; (b) stage 2; and (c) stage 3.

During stage 1, fire has just occurred, and the fire source heats up the gas inside the tunnel, causing the volume of gas inside the tunnel to expand. A small quantity of air is evacuated from each shaft and tunnel portal at this time. The flow direction of each outlet is toward the outside of the tunnel.

During stage 2, the smoke front passes through the first vertical shaft and spreads toward the second vertical shaft. Some of the smoke starts to be extracted from the first shaft, and according to the principle of mass conservation, the second to fifth shafts and the tunnel portal become air supply. At this time, except for the first shaft, which is in the smoke extraction state, all other openings are in the air intake state. Changes in airflow occur due to the influence of both the position and cross-sectional size of the opening, thus affecting the mass flow rate of air supply.

During stage 3, smoke flows through two vertical shafts and is completely exhausted from the tunnel. The smoke propagation within the tunnel remains steady, with a constant mass flow rate of smoke extraction by each shaft. At this time, the first and second shafts are in the smoke extraction state, while the third to fifth shafts and the tunnel portal are in the air supply state.

During the stable development stage of smoke, which is stage 3, smoke is expelled through vertical shafts 1 and 2. The reduction in mass inside the tunnel creates a pressure difference between the tunnel's interior and exterior. This pressure differential leads to the generation of air supply through vertical shafts 3, 4, and 5. In accordance with the principle of mass conservation, the total mass flow rate of smoke discharged from the tunnel equals the total mass flow rate of air entering the tunnel, as represented by Equation (1):

$$M_1 + M_2 = M_3 + M_4 + M_5 + M_0 \tag{1}$$

where M is the mass flow rate (kg/s), 1~5 are the serial numbers of the vertical shafts, 0 is the tunnel portal.

Vertical shafts 3, 4, and 5, along with the roadway, form a coherent ventilation network that facilitates airflow. Since each vertical shaft and the tunnel portal are open to the external environment, the pressures in these areas remain equalized. Therefore, these various vertical shafts and the lane of the tunnel can be considered as a parallel ventilation network. According to the principle stating that the wind pressure of parallel air paths in a ventilation network is equal, the following equation can be derived:

$$R_{F,d/2}M_0^2 = (R_{L,shaft5} + R_{F,shaft5})M_5^2 \tag{2}$$

$$R_{F,d/2}M_0^2 + R_{F,d}(M_0 + M_5)^2 = (R_{L,shaft4} + R_{F,shaft4})M_4^2 \tag{3}$$

$$R_{F,d/2}M_0^2 + R_{F,d}(M_0 + M_5)^2 + R_{F,d}(M_0 + M_4 + M_5)^2 = (R_{L,shaft3} + R_{F,shaft3})M_3^2 \tag{4}$$

where R is the ventilation resistance (kg/(s·m⁴)), F is the frictional resistance, and d is the distance between shafts (m).

The Atkinson equation is a well-known method to determine the pressure drop in airways [17], which is determined as follows:

$$\Delta P = RV^2 \tag{5}$$

In the preceding equation, the frictional resistance of the shafts and the tunnel can be calculated as follows [18]:

$$h_{F,lane} = R_{F,lane}M_{lane}^2 = \frac{\lambda\rho_0 L_{lane} U_{lane}}{8S_{lane}^3} \left(\frac{M_{lane}}{\rho_\infty} \right)^2 \tag{6}$$

$$h_{F,shaft} = R_{F,shaft}M_{shaft}^2 = \frac{\lambda\rho_0 L_{shaft} U_{shaft}}{8S_{shaft}^3} \left(\frac{M_{shaft}}{\rho_\infty} \right)^2 \tag{7}$$

where λ is the coefficient of resistance along the course, ρ_∞ is the ambient density (kg/m³), L is the length (m), U is the perimeter of the tunnel cross section (m), and S is the tunnel cross-sectional area (m²).

The local resistance of air flowing from a shaft to the tunnel, where the flow direction changes from vertical to horizontal, can be expressed as follows:

$$h_{L,shaft} = R_{L,shaft}M_{shaft}^2 = \xi \frac{M_{shaft}^2}{2\rho_\infty S_{shaft}^2} \tag{8}$$

where ξ is the local resistance loss coefficient.

These unknowns that need to be solved involve 4 parameters, including 3 shafts and a tunnel port, so we need to solve four equations, i.e., 1–4, and R_F and R_L are obtained from the calculations based on Equations (5)–(7).

3. Numerical Simulation

The numerical simulations for this work were carried out via a high-performance computer cluster utilizing the Fire Dynamic Simulator (FDS). Numerous previous studies have demonstrated its dependability [19–25].

The numerical simulation model of the tunnel, as presented in this paper, is grounded in the actual construction of the Nanjing Tongjimen Tunnel. The air supply behavior examined herein represents a special smoke movement phenomenon identified by the tunnel operation management units during fire response procedures. The concrete tunnel model in Figure 2 has dimensions of 600 m (length) × 12 m (width) × 6 m (height). The vertical shafts were strategically placed at 60 m intervals along the tunnel’s central axis in the longitudinal direction. The width of the vertical shafts was fixed at 3 m, while the height and length were adjusted according to the specific test conditions. Both the tunnel and shaft ends were configured as “OPEN.” The external temperature was maintained at 20 °C. The air density was 1.29 kg/m³ and the ambient pressure was 1.01325 Pa. The fire source was centrally positioned within the tunnel, while the mass flow devices were installed at both ends of the tunnel and above each shaft. The simulation duration spanned 600 s.

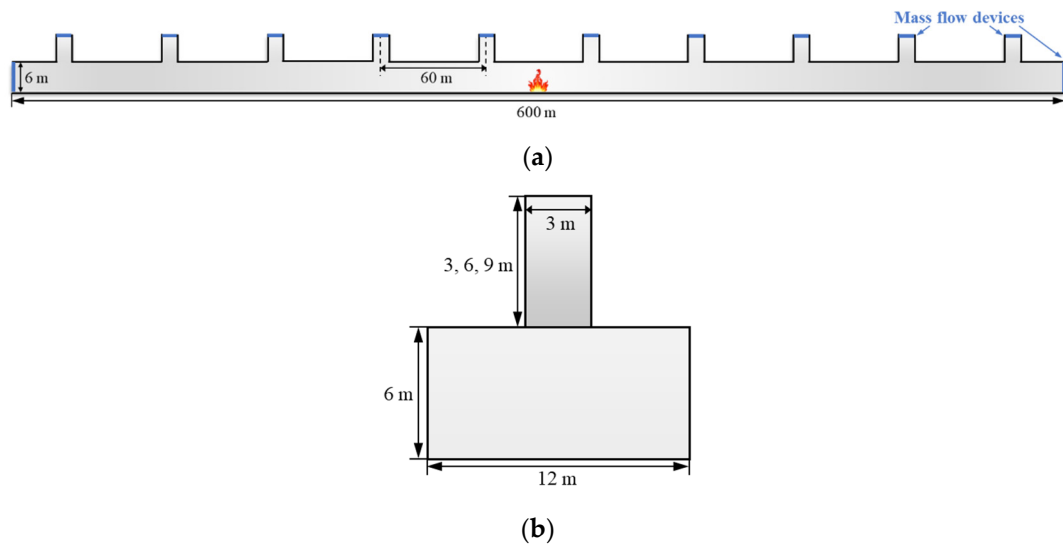


Figure 2. Tunnel model schematic: (a) forward perspective and (b) lateral perspective.

3.1. Fire Scenarios

This study examines smoke flow under different conditions, including a selection of three HRRs (1 MW, 2 MW, and 5 MW), which represent typical vehicle fires involving 1–3 passenger cars [26], two fire growth rates (immediate and fast), three shaft heights (3 m, 6 m, and 9 m), and three shaft lengths (2 m, 4 m, and 6 m). Table 1 outlines the specific working conditions in detail.

Table 1. Test conditions.

No.	HRR (MW)	Ramp-Up Time (s)	Sizes of Shafts: Height (m) × Length (m)
1–3	1, 2, 5	0	6 × 6
4–5	5	0, 325	6 × 6
			3 × 2
			3 × 4
6–10	5	0	3 × 6
			6 × 6
			9 × 6

3.2. Grid Independence Analysis

The selection of grid size significantly influences the outcomes of simulations, as highlighted in the *FDS Handbook* [27]; hence, $D^*/16 \sim D^*/4$ should be between 4 and 16, where D^* can be determined as follows:

$$D^* = \left(\frac{\dot{Q}}{\rho_\infty C_p T_\infty \sqrt{g}} \right)^{\frac{2}{5}} \tag{9}$$

This study selected the grid size of 0.125 m × 0.125 m × 0.125 m, which was brought into Equation (9). Table 2 presents the calculation results of D^* and D^*/D at various HRRs, indicating that the chosen size in this simulation was appropriate.

Table 2. The calculation results of D^* and D^*/D .

HRR (MW)	D^*	D^*/D
1	0.959027	7.672216
2	1.265443	10.123549
5	1.825655	14.605244

4. Results and Interpretation

4.1. Smoke Spread Characteristics under Natural Ventilation Using Multiple Vertical Shafts

In the test conditions described in this article, smoke propagation exhibits similarity. After traversing two vertical shafts, smoke is almost extracted from the tunnel. The smoke temperature distribution is illustrated in Figure 3, while Figure 4 depicts the vertical flow velocity distribution, both based on test condition 3. Figure 3 shows the spread range of smoke at different time intervals, while Figure 4 visualizes the flow direction within various vertical shafts, with upward flow represented as orange and downward flow indicated in blue. By comparing Figures 3 and 4, at around 10 s, the smoke front is about to reach the first vertical shaft. At this time, the first and second shafts appear orange, indicating that gas is being discharged from inside to outside the tunnel, which is consistent with the previous theoretical analysis. Due to the low wind speed inside vertical shafts 3, 4, and 5, it is not depicted in Figure 4. The smoke front passes through the first vertical shaft at 50 s, causing smoke to exit from it. Vertical shafts 2, 3, and 4 are indicated by a blue color, indicating the inflow of cold air from outside the tunnel. In contrast, the first vertical shaft exhibits a mixture of blue and orange colors due to the presence of vortices caused by the smoke exhaust flow not reaching its maximum value yet. At 150 s, smoke flows through the second vertical shaft, and at around 250 s, the spread range of smoke stabilizes and no longer changes. At this time, vertical shafts 1 and 2 appear orange, indicating that smoke is being discharged, and vertical shafts 3, 4, and 5 appear blue, indicating that an air supply has formed.



Figure 3. Temperature distribution diagram in the tunnel.

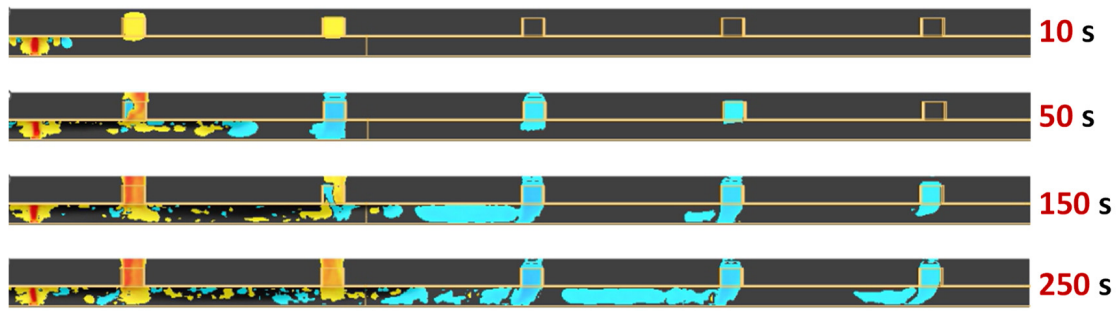


Figure 4. Vertical velocity distribution diagram in the tunnel.

The gas flow direction in vertical shaft 2 changes three times during the smoke spreading process. The internal flow field provides a clear depiction of the evolving pattern during the three stages of the fire. A local cutout of vertical shaft 2, as illustrated in Figure 5, enables the observation of these changes.

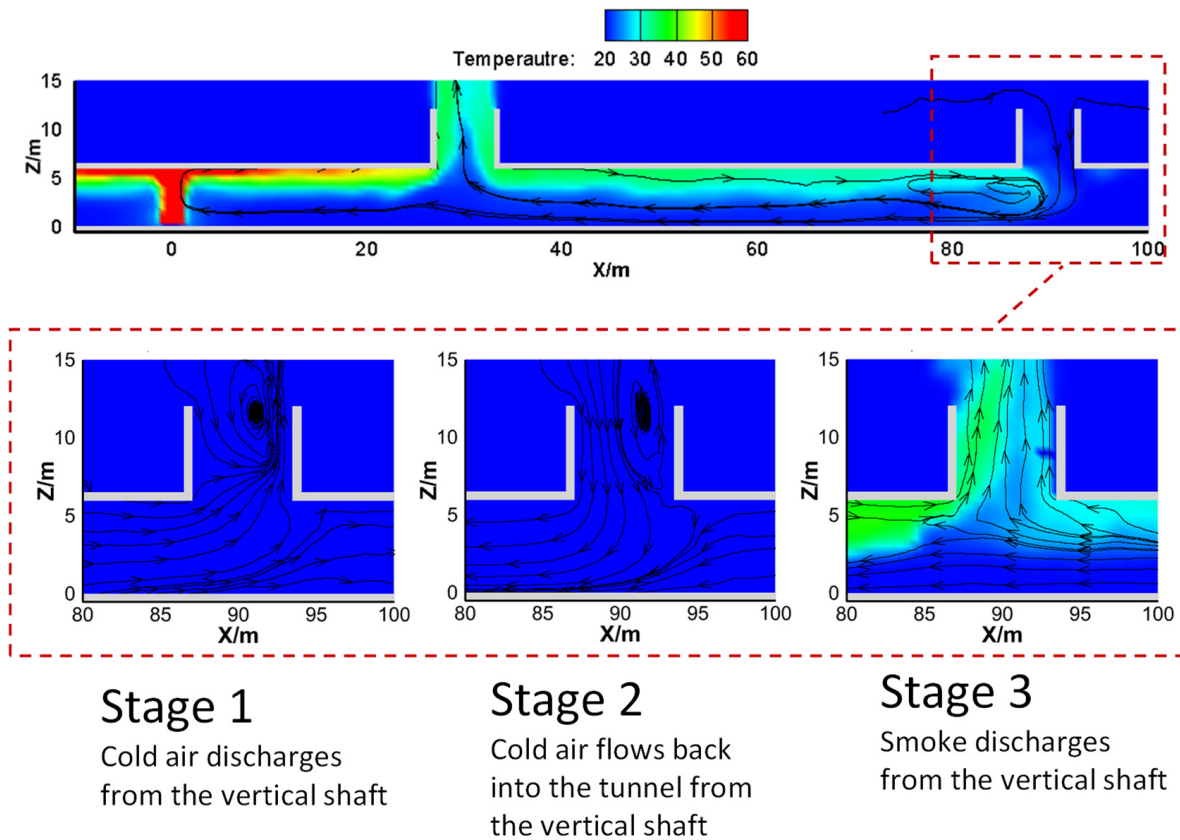


Figure 5. Flow field distribution patterns of vertical shaft 2 in different stages.

In the initial stage of the fire, before the smoke front reaches vertical shaft 1, the gas expands inside the tunnel and is expelled through multiple openings. Consequently, the gas flow direction in shaft 2 is outward.

When the smoke front flows through vertical shaft 1, each opening presents the function of supplying air, and cold air flows into the tunnel through vertical shaft 2 and other vertical shafts or the tunnel portal. At this time, the gas flow direction in vertical shaft 2 is downward.

Upon the smoke front reaching vertical shaft 2, smoke starts to flow out of the tunnel via this shaft. Consequently, the gas flow direction within vertical shaft 2 undergoes a change once again.

When smoke in a tunnel has spread over a long distance, the temperature drops significantly, buoyancy is weakened, and smoke will be precipitated [28,29]. However, as shown in Figure 5, smoke in the tunnel before its discharge still has a strong buoyancy to maintain its stable stratification. Thus, the sink part has a weak effect and is not considered.

4.2. Factors Influencing Smoke/Air Mass Flow Rate in Vertical Shafts

(1) HRR

The heat release rate (HRR) exerts a significant influence on natural ventilation within vertical shafts. Higher HRR levels lead to increased mass flow rates of gas and smoke velocity. As depicted in Figure 6a, the smoke exhaust mass flow rate of vertical shaft 1 experiences a rapid increase upon the fire’s ignition and eventually stabilizes at a constant level. Vertical shaft 1 demonstrates higher smoke exhaust mass flow rates and quicker attainment of a steady state with higher HRRs. Similarly, vertical shaft 2 exhibits a comparable trend but attains lower steady-state smoke exhaust mass flow rates due to its increased distance from the fire source. Additionally, vertical shaft 2 needs a longer duration to reach a stable state after the initiation of the fire.

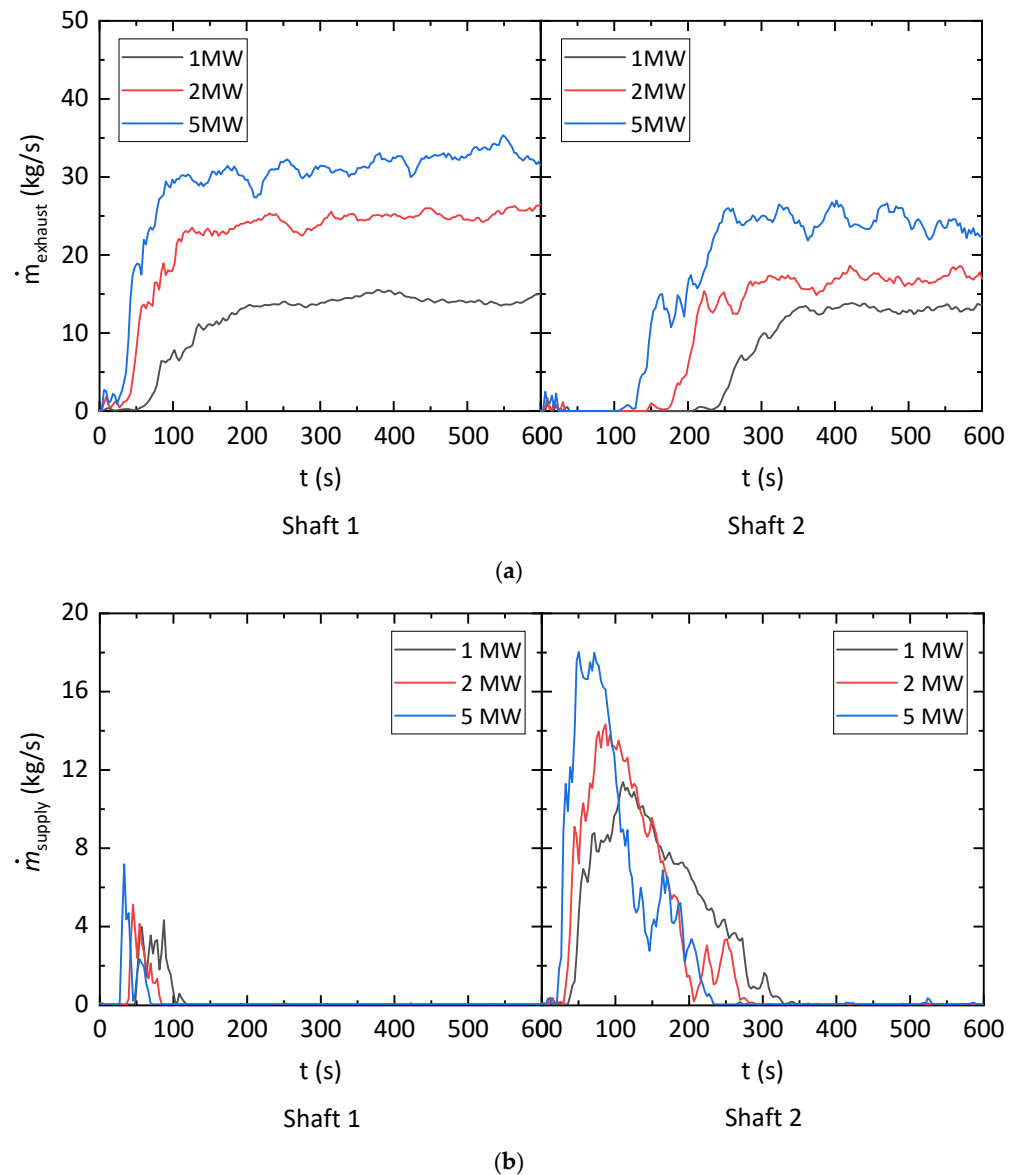


Figure 6. Mass flow rate of smoke exhaust and air supply in shafts 1 and 2 at different HRRs: (a) smoke exhaust and (b) air supply.

The mass flow rates of smoke exhaust and air supply of vertical shafts 1 and 2 vary significantly. According to the theoretical analysis, when vertical shaft 1 starts to exhaust smoke, the air supply in vertical shaft 2 increases dramatically. As the smoke front reaches vertical shaft 2, the air supply in vertical shaft 2 decreases dramatically, and its state changes from air supply to smoke exhaust. It is worth noting that in the initial stages, as shown in Figure 6b, vertical shaft 1 experiences inadequate air supply. This phenomenon can be attributed to the positioning of the measurement slice of gas mass flow rate at the upper portion of the shafts, as observed in the simulation results. When the smoke front traverses the shafts, the exhaust mass flow rate reaches its maximum, leading to the development of a boundary layer within the vertical shafts. As shown in Figure 6a, the boundary layer triggers the formation of eddies and enables a slight infiltration of smoke from the external environment into the vertical shafts. Once the smoke front completely passes through vertical shaft 1, the exhaust mass flow rate attains its peak value, resulting in the cessation of air supply within vertical shaft 1.

(2) fire growth rate

Fire growth rate is a significant parameter that cannot be ignored in real fires, which are typically considered as slow, medium, and fast fires, corresponding to different growth rates. In test condition 4, the HRR of the fire gradually increases until it reaches its peak. After 325 s, the fire reaches its peak power of 5 MW, following a fire development rate of 0.0469 kW/s^2 , as demonstrated in test condition 5.

In Figure 7a, the development rate of the fire has no impact on steady-state exhaust smoke in the shafts. The main effect of the fire growth rate is that a slower rate results in a longer time for the shafts to reach their maximum exhaust rate in mass flow and a slower smoke front velocity. The start time for smoke exhaust in shaft 2 is also significantly delayed compared to the case of a smaller fire growth rate.

In Figure 7b, the fire growth rate significantly delays the start and end times of air supply in the shafts. It is worth noting that a higher fire growth rate leads to a slightly lower maximum mass flow rate in air supply in shaft 2.

(3) shaft size

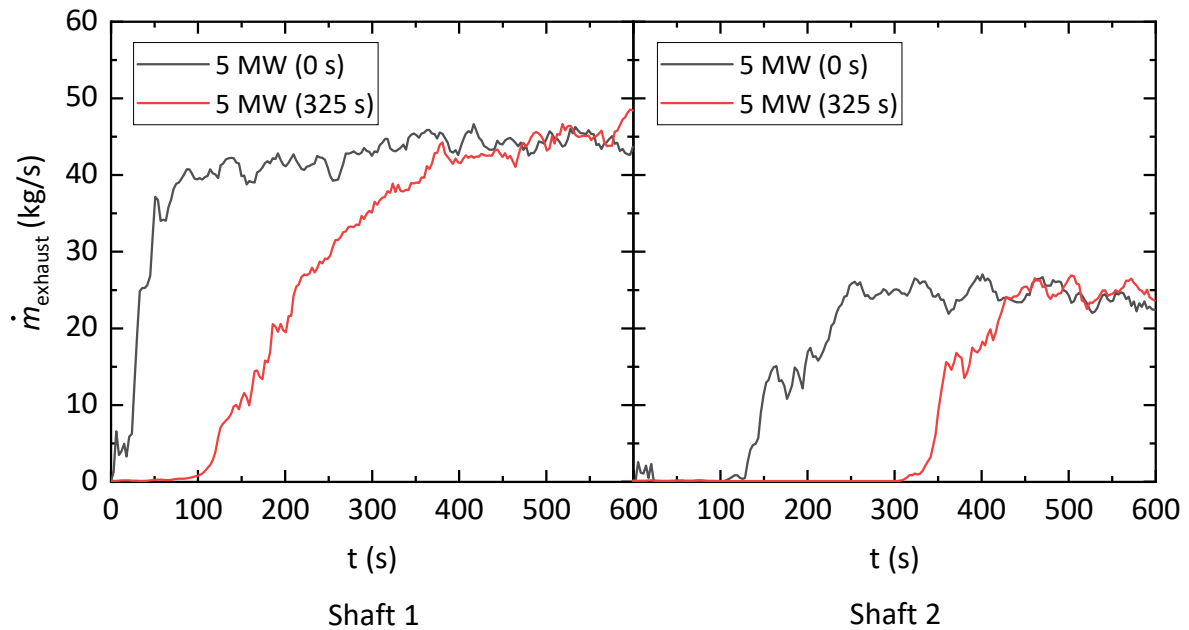
This study primarily focuses on the impact of varying shaft heights and lengths. As shown in Figure 8a, the cross-sectional area of the shafts is positively correlated with the smoke exhaust rate as the shaft length increases. However, the growth rate of the smoke exhaust rate is not affected by the increase in shaft section. Furthermore, the longer shafts effectively enhance the smoke exhaust rate via an improved chimney effect. Notably, as the smoke exhaust rate of shaft 1 increases, the commencement of smoke exhaust in shaft 2 gradually experiences a delay, signifying a deceleration in the smoke front's speed. Overall, we could say that the smoke exhaust capacity increases with a rise in length and height of shafts to a certain extent.

The smoke exhaust of shaft 1 has a direct impact on the air supply requirement of shaft 2, resulting in a reduced smoke front flow rate and an extended duration of air supply to shaft 2. Furthermore, the size of the shaft influences the vortex formation at the shaft opening, with shorter shafts experiencing a more pronounced vortex effect. Throughout the simulation, the gas mass flow rate of shaft 1 was continuously monitored. When designing a shaft exhaust system, it is essential to take into account the potential drawbacks of shorter shafts and mitigate any interference they may cause in the effectiveness of smoke exhaust due to vortex formation.

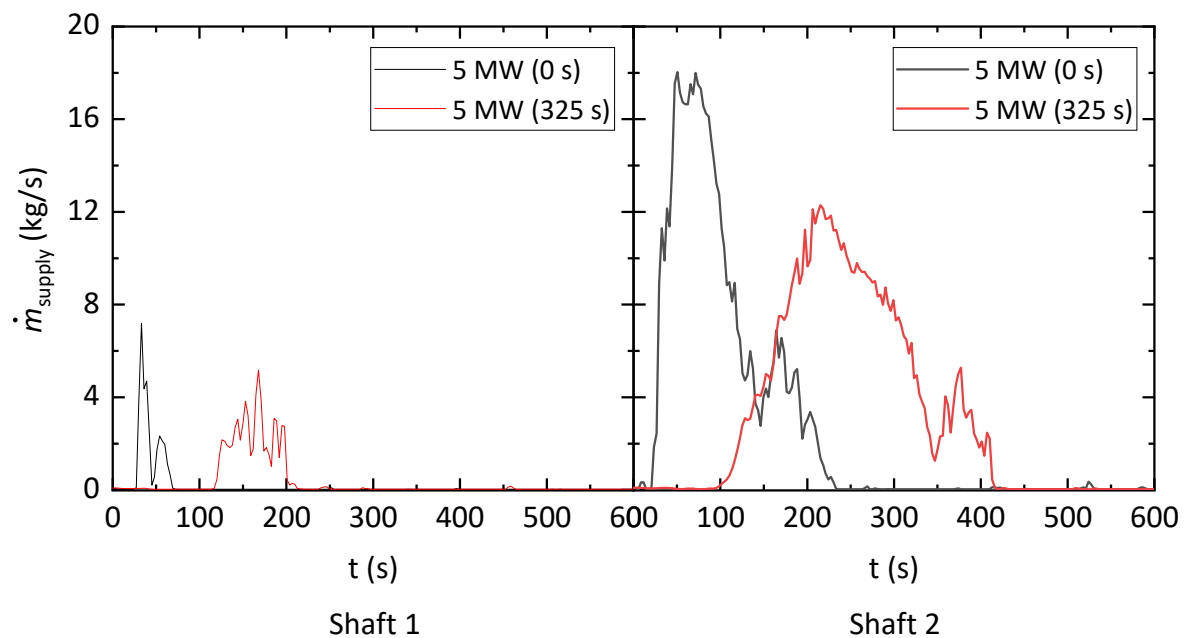
4.3. Prediction of Air Supply Mass Flow Rate for Natural Smoke Extraction with Multiple Vertical Shafts

According to the predictive model discussed in the previous section, this section presents the predictions at different HRRs (1 MW, 2 MW, and 5 MW). In these test conditions, once the fire reaches a stable stage, the smoke front no longer moves after passing through smoke exhaust shafts 1 and 2. Therefore, smoke is exhausted through shafts 1 and 2, while shafts 3, 4, and 5 and the tunnel portal requires additional air supply. The model was used

to anticipate the air supply mass flow for shafts 3, 4, and 5, as well as the tunnel portal. To assess the predictive model's accuracy, the total air supply mass flow rate used as the input was determined by calculating the smoke exhaust mass flow rate of shafts 1 and 2, following the principle of mass conservation outlined in Equation (1). This ensures that the mass flow rate of air entering the tunnel through the shafts or the portal is equivalent to that of smoke, allowing for a comprehensive comparison of the predictive model's effectiveness.



(a)



(b)

Figure 7. Smoke exhaust and air supply in mass flow rate of shafts 1 and 2 at various fire growth rates: (a) smoke exhaust and (b) air supply.

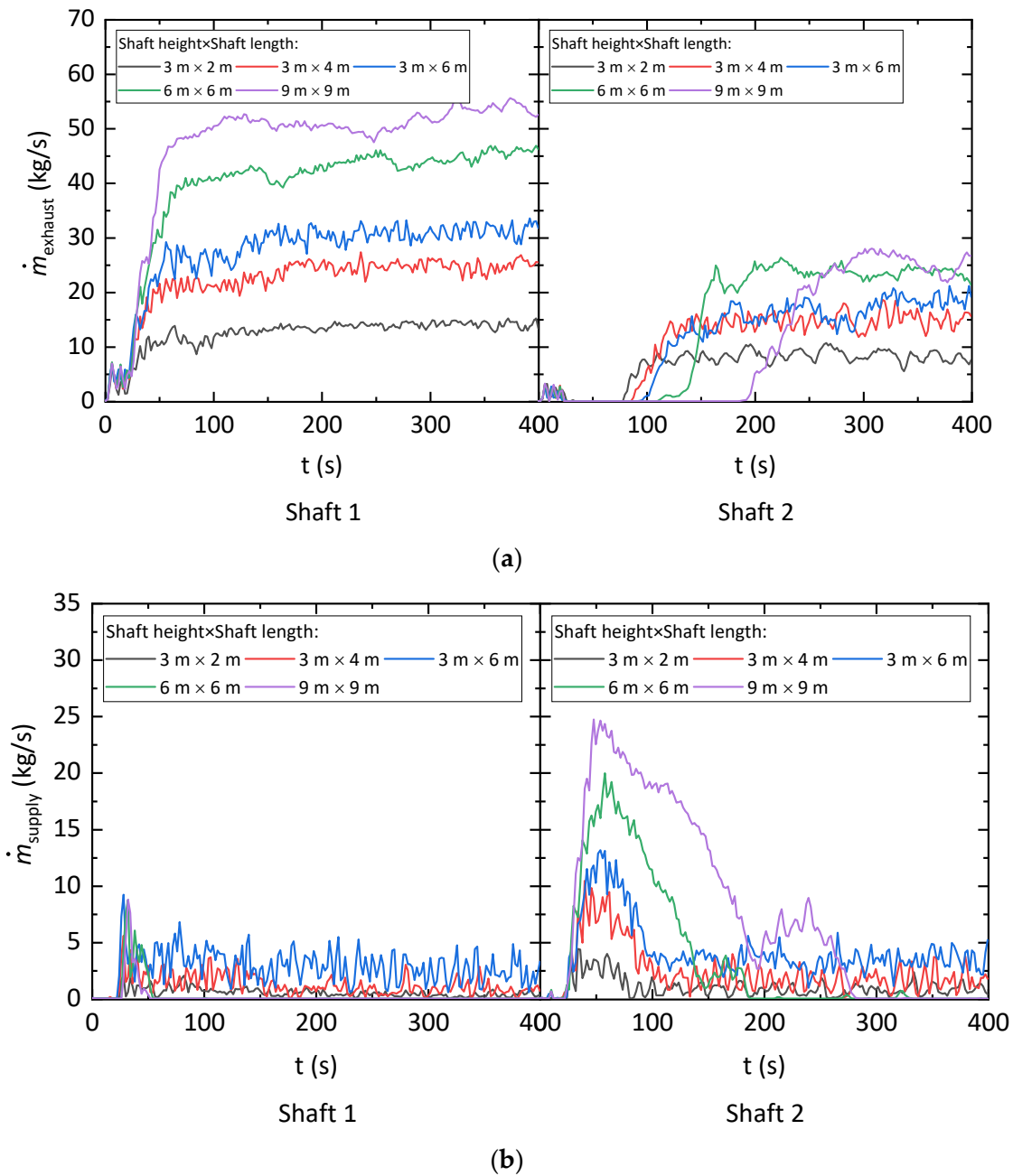


Figure 8. Mass flow rate of smoke exhaust and air supply in shafts 1 and 2 for shafts of different sizes: (a) smoke exhaust and (b) air supply.

Figure 9 shows the percentage of supply air flow to each shaft/portal to the total supply air flow at various HRRs. It can be seen that the percentage of air flow through the shafts decreases gradually toward the portal. The majority of air flow enters the tunnel through the portal. At the same time, the supply air flow is basically not influenced by HRRs.

Figure 10 demonstrates the reliable performance of the predictive model in estimating the air supply mass flow rate for both smoke exhaust shafts and the tunnel portal across various HRRs. The predicted values closely align with the simulated values. The smaller cross-sectional area of the shafts, compared to the tunnel roadway, reduces frictional resistance and leads to a higher air supply mass flow rate through the tunnel portal. The position of each exhaust shaft relative to the fire source influences its air supply. Shaft located farther from the fire source encounter greater resistance, leading to lower air supply

mass flow rates compared to shafts closer to the fire source. The correlation is effectively captured by both the predicted and simulated values.

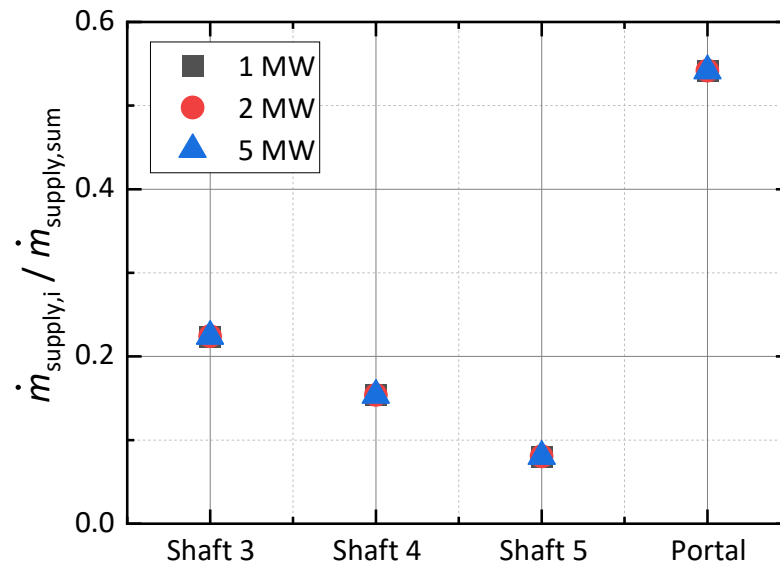


Figure 9. Percentage of supply air flow to each shaft/portal to the total supply air flow under different HRR conditions.

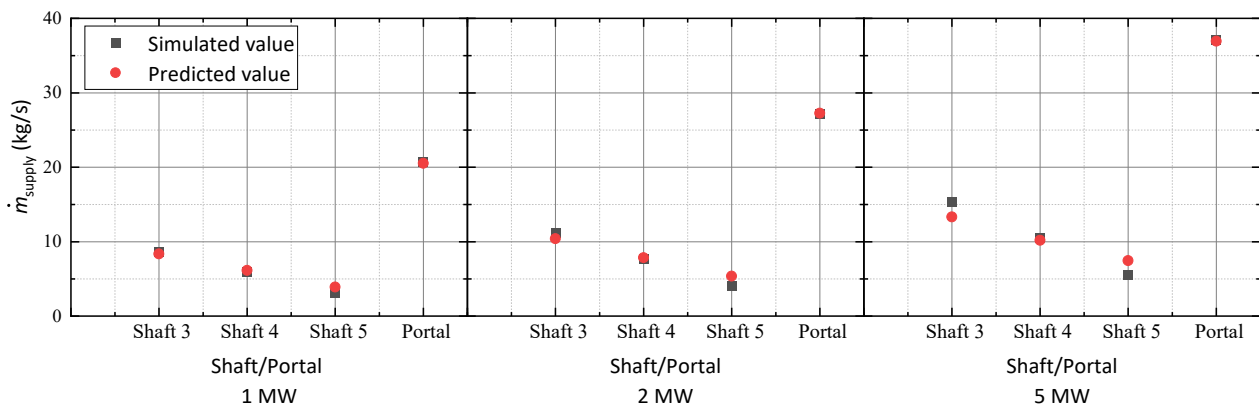


Figure 10. Comparison of simulated and predicted air supply flow rates from shaft/portal at different HRRs.

5. Conclusions

Numerical simulations were conducted in this study to analyze the flow field propagation within a tunnel during a fire under a multi-shaft natural ventilation system. This study focused on identifying factors that influence air supply, analyzing the characteristics of shaft air supply during different fire development stages, and assessing how various factors influence the tunnel’s flow field. Additionally, a predictive model was developed to estimate the air supply mass flow rate in shafts during the steady growth phase of a fire. Since temperature, air density, and other data used in this study are not the same as those in an actual fire, it may lead to inaccurate prediction results. The specific conclusions derived from this study are as follows:

- (1) In a multi-shaft ventilation tunnel during a fire, certain shafts are responsible for smoke extraction, while other shafts and tunnel portals not involved in smoke removal provide an air supply. The air supply mass flow rate in the shafts is impacted by various factors, including shaft dimensions and the overall tunnel structure.

- (2) The mass flow rates of smoke exhaust and air supply increase as the HRR rises. A slower growth rate of the fire source results in a longer duration of air supply and a lower maximum mass flow rate. Additionally, shafts with larger cross-sectional areas or greater heights demonstrate higher smoke extraction capacities, thus requiring a greater air supply.
- (3) Each shaft and tunnel portal has an inflow air supply mass flow rate that matches the discharge rate of hot smoke. The magnitude of inflow air supply in each shaft is determined by its proximity to the fire source. The proposed predictive model, developed based on the ventilation network theory, accurately estimates natural smoke extraction in multi-shaft setups, with its estimates aligning with the numerical simulation outcomes.

Author Contributions: Investigation, L.H., K.L., H.Z., C.J. and H.T.; Writing—Review & Editing, L.H., Y.M. and G.Z.; Visualization, Y.M. All authors have read and agreed to the published version of the manuscript.

Funding: This study was funded by the National Natural Science Foundation of China (NSFC) under Grant No. 52204252; The Science Foundation of National Fire and Rescue Administration of China under Grant No. 2023XFCX16; and The Fundamental Research Funds for the Central Universities under Grant No. 2022ZZCX05K02.

Institutional Review Board Statement: Not applicable.

Informed Consent Statement: Not applicable.

Data Availability Statement: The data that support the findings of this study are available from the corresponding author upon reasonable request.

Acknowledgments: This study was funded by the National Natural Science Foundation of China (NSFC) under Grant No. 52204252, Science Foundation of National Fire and Rescue Administration of China under Grant No. 2023XFCX16 and the Fundamental Research Funds for the Central Universities under Grant No. 2022ZZCX05K02. The authors gratefully appreciate all these supports.

Conflicts of Interest: The authors declare no conflict of interest.

Nomenclature

M	mass flow rate (kg/s)
$\dot{m}_{exhaust}$	mass flow rate of smoke exhaust (kg/s)
\dot{m}_{supply}	mass flow rate of air supply (kg/s)
R	ventilation resistance (kg/(s·m ⁴))
h	pressure drop (Pa)
L	length (m)
U	perimeter of tunnel cross section (m)
\dot{Q}	heat release rate (MW)
g	gravitational acceleration (m/s ²)
S	tunnel cross-sectional area (m ²)
ρ	density (kg/m ³)
D^*	diameter of fire source (m)
T	temperature (K)
C_p	isobaric heat capacity (kJ/(kg·K))
λ	coefficient of resistance along the course
ξ	coefficient of local resistance loss
SUBSCRIPT	
1~5	serial number of vertical shafts
0	tunnel portal
F	frictional resistance
L	local resistance
∞	ambient

References

1. Ren, R.; Zhou, H.; Hu, Z.; He, S.; Wang, X. Statistical analysis of fire accidents in Chinese highway tunnels 2000–2016. *Tunn. Undergr. Space Technol.* **2019**, *83*, 452–460. [[CrossRef](#)]
2. Beard, A.; Carvel, R. *The Handbook of Tunnel Fire Safety*; Thomas Telford Publishing: London, UK, 2005; ISBN 978-0-7277-3875-2.
3. Liu, D.; Xu, Z.; Fan, C.; Zhou, Y. Development of fire risk visualization tool based on heat map. *J. Loss Prev. Process Ind.* **2021**, *71*, 104505. [[CrossRef](#)]
4. Ingason, H.; Li, Y.Z.; Lönnemark, A. *Tunnel Fire Dynamics*; Springer: New York, NY, USA, 2015; ISBN 978-1-4939-2198-0.
5. Ji, J.; Gao, Z.H.; Fan, C.G.; Zhong, W.; Sun, J.H. A study of the effect of plug-holing and boundary layer separation on natural ventilation with vertical shaft in urban road tunnel fires. *Int. J. Heat Mass Transf.* **2012**, *55*, 6032–6041. [[CrossRef](#)]
6. Ji, J.; Fan, C.G.; Gao, Z.H.; Sun, J.H. Effects of vertical shaft geometry on natural ventilation in urban road tunnel fires. *J. Civ. Eng. Manag.* **2014**, *20*, 466–476. [[CrossRef](#)]
7. Fan, C.G.; Ji, J.; Gao, Z.H.; Han, J.Y.; Sun, J.H. Experimental study of air entrainment mode with natural ventilation using shafts in road tunnel fires. *Int. J. Heat Mass Transf.* **2013**, *56*, 750–757. [[CrossRef](#)]
8. Fan, C.G.; Ji, J.; Wang, W.; Sun, J.H. Effects of vertical shaft arrangement on natural ventilation performance during tunnel fires. *Int. J. Heat Mass Transf.* **2014**, *73*, 158–169. [[CrossRef](#)]
9. Cong, H.; Wang, X.; Kong, X.; Xu, H. Effects of fire source position on smoke extraction efficiency by natural ventilation through a board-coupled shaft during tunnel fires. *Proc. Combust. Inst.* **2019**, *37*, 3975–3984. [[CrossRef](#)]
10. He, L.; Xu, Z.; Markert, F.; Zhao, J.; Liu, Q.; Tao, H.; Wang, Z.; Fan, C. Experimental study of heat exhaust efficiency with natural ventilation in tunnel fire: Impact of shaft height and heat release rate. *J. Wind Eng. Ind. Aerodyn.* **2020**, *201*, 104173. [[CrossRef](#)]
11. Guo, Q.; Zhu, H.; Yan, Z.; Zhang, Y.; Zhang, Y.; Huang, T. Experimental studies on the gas temperature and smoke back-layering length of fires in a shallow urban road tunnel with large cross-sectional vertical shafts. *Tunn. Undergr. Space Technol.* **2019**, *83*, 565–576. [[CrossRef](#)]
12. Guo, Q.; Zhu, H.; Zhang, Y.; Shen, Y.; Zhang, Y.; Yan, Z. Smoke flow in full-scale urban road tunnel fires with large cross-sectional vertical shafts. *Tunn. Undergr. Space Technol.* **2020**, *104*, 103536. [[CrossRef](#)]
13. Guo, Q.; Zhu, H.; Zhang, Y.; Yan, Z. Theoretical and experimental studies on the fire-induced smoke flow in naturally ventilated tunnels with large cross-sectional vertical shafts. *Tunn. Undergr. Space Technol.* **2020**, *99*, 103359. [[CrossRef](#)]
14. Li, Z.; Jiang, H.; Cheng, Y.; Gao, Y.; Chen, L.; Zhang, Y.; Li, T.; Xing, S. Effects of longitudinal fire source locations on the maximum temperature and longitudinal temperature decay in a mountain tunnel with vertical shaft: An experimental investigation and empirical model. *J. Therm. Anal. Calorim.* **2022**, *147*, 12139–12154. [[CrossRef](#)]
15. Wang, Z.; Deng, W.; Zhou, M.; Fang, Z.; Guan, Y.; Tang, Z. Evaluation of fire smoke and heat exhaust performance of shafts by natural venting in tunnels. *Tunn. Undergr. Space Technol.* **2023**, *131*, 104817. [[CrossRef](#)]
16. Fan, C.; Bu, R.; Xie, X.; Zhou, Y. Full-scale experimental study on water mist fire suppression in a railway tunnel rescue station: Temperature distribution characteristics. *Process Saf. Environ. Prot.* **2021**, *146*, 396–411. [[CrossRef](#)]
17. Amiri, L.; Ghoreishi-Madiseh, S.A.; Hassani, F.P.; Sasmito, A.P. Friction factor correlation for airflow through broken rocks and its applications in mine ventilation. *Int. J. Min. Sci. Technol.* **2020**, *30*, 455–462. [[CrossRef](#)]
18. Mcpherson, M.J. *Subsurface Ventilation and Environmental Engineering*; Springer: Dordrecht, The Netherlands, 1993.
19. Chow, W.K.; Gao, Y.; Zou, J.F.; Liu, Q.K.; Chow, C.L.; Miao, L. Numerical Studies on Thermally-Induced Air Flow in Sloping Tunnels with Experimental Scale Modelling Justifications. *Fire Technol.* **2018**, *54*, 867–892. [[CrossRef](#)]
20. Gannouni, S.; Maad, R.B. Numerical study of the effect of blockage on critical velocity and backlayering length in longitudinally ventilated tunnel fires. *Tunn. Undergr. Space Technol.* **2015**, *48*, 147–155. [[CrossRef](#)]
21. Huang, Y.; Li, Y.; Dong, B.; Li, J.; Liang, Q. Numerical investigation on the maximum ceiling temperature and longitudinal decay in a sealing tunnel fire. *Tunn. Undergr. Space Technol.* **2018**, *72*, 120–130. [[CrossRef](#)]
22. Liu, C.; Zhong, M.; Tian, X.; Zhang, P.; Xiao, Y.; Mei, Q. Experimental and numerical study on fire-induced smoke temperature in connected area of metro tunnel under natural ventilation. *Int. J. Therm. Sci.* **2019**, *138*, 84–97. [[CrossRef](#)]
23. Liu, Q.; Xu, Z.; Fan, C.; Tao, H.; Zhao, J.; He, L. Experimental and Numerical Study of Plug-Holing with Lateral Smoke Exhaust in Tunnel Fires. *Fire Technol.* **2022**. [[CrossRef](#)]
24. Tian, X.; Liu, C.; Zhong, M. Numerical and experimental study on the effects of a ceiling beam on the critical velocity of a tunnel fire based on virtual fire source. *Int. J. Therm. Sci.* **2021**, *159*, 106635. [[CrossRef](#)]
25. Wang, Z.; Jiang, X.; Park, H.; Wang, L.; Wang, J. Numerical Investigation on the length of the near-field region of smoke flow in tunnel fires. *Case Stud. Therm. Eng.* **2021**, *28*, 101584. [[CrossRef](#)]
26. Ko, J.; Yoon, C.; Yoon, S.; Kim, J. Determination of the applicable exhaust airflow rate through a ventilation shaft in the case of road tunnel fires. *Saf. Sci.* **2010**, *48*, 722–728. [[CrossRef](#)]
27. McGrattan, K.B.; Forney, G.P. *Fire Dynamics Simulator: User's Guide*, 6th ed.; National Institute of Standards and Technology: Gaithersburg, MD, USA, 2004.

28. Lin, P.; Wang, Z.-K.; Wang, K.-H.; Gao, D.; Shi, J.-K.; You, S.-H.; Chen, Z.-N.; Wang, G.-Y.; Mei, X.-J. An experimental study on self-extinction of methanol fire in tilted tunnel. *Tunn. Undergr. Space Technol.* **2019**, *91*, 102996. [[CrossRef](#)]
29. Lin, P.; Zuo, C.; Xiong, Y.; Wang, K.; Shi, J.; Chen, Z.; Lu, X. An experimental study of the self-extinction mechanism of fire in tunnels. *Tunn. Undergr. Space Technol.* **2021**, *109*, 103780. [[CrossRef](#)]

Disclaimer/Publisher's Note: The statements, opinions and data contained in all publications are solely those of the individual author(s) and contributor(s) and not of MDPI and/or the editor(s). MDPI and/or the editor(s) disclaim responsibility for any injury to people or property resulting from any ideas, methods, instructions or products referred to in the content.